YITP-04-7

Continuous Color-Flavor Unlocking Transition

Hiroaki Abuki

Yukawa Institute for Theoretical Physics, Kyoto University, Kyoto, Japan

(Dated: May 22, 2019)

Abstract

We revisit the unlocking transition from the color-flavor locked phase to the two-flavor pairing phase paying a special attention to the multiplicity of the gap parameters and the density of strange quark. By deriving the exact effective potential for the multi-gap parameters, we show that the unlocking transition at zero temperature is of 2nd order rather than of 1st order. Furthermore, the CFL phase is much more robust against the increase of the strange quark mass than is predicted by the kinematical criterion for the unlocking. In fact, the critical mass M_s^c is controlled not by the magnitude of the gap at zero temperature but by the strange quark density. The fact of $M_s^c > 0$ strongly supports the realization of Bose-Einstein condensation of tightly bound pairs composed of strange quark and (u,d) quarks at low strange quark density. We also find the fact that the color-flavor locking state actually corresponds to a saddle point of the effective potential, which is unstable in the three out of five directions.

PACS numbers: 12.38.-t, 12.38.Aw, 25.75.Nq

I. INTRODUCTION

Since a possible color superconducting phase was proposed by Bailin and Love [1], the dynamics of QCD under high baryon density has been attracted much interests [2] and is revealing its rich and interesting phase structures [3]. In particular, the color-flavor locked (CFL) type of the pairing order [4] is most likely to emerge at sufficiently high quark chemical potential μ for relatively small strange quark mass M_s. In contrast to this solid fact, however, the phases for larger and realistic value of M_s^2/μ are not uncovered yet, and so many phases have been proposed and various phase transitions have been studied so far: These include: the simple scenario of the unlocking transition from the CFL to the two-flavor ordering (2SC) state [5, 6], the inhomogeneous LOFF (Larkin-Ovchinnikov-Fulde-Ferrell) type of the pairing state [7, 8], the CFL state with kaon (K^0, K^+) condensation [9], the gapless 2SC state [10] and its CFL version [11], and dSC state [12], and which phase to be favored for realistic value of M_s remains a still controversial problem.

The unlocking transition from the CFL state to the 2SC state with increasing the value of M_s^2/μ is firstly investigated using Nambu–Jona-Lasinio (NJL) type effective models [5, 6]. Their results show that as the strange quark mass is increased, the 1st order unlocking transition takes place at some critical M_s^c, and a simple kinematical criterion for the critical mass works quite well. This criterion is based on the observation that the transition from the CFL to the 2SC with increasing M_s would occur when the mismatch of the Fermi momenta of light and strange quark becomes as large as the magnitude of the gap. In Ref. [5], the fermionic dispersions are approximately constructed by the expansion in the flavor breaking parameter M_s^2/μ, and after that, the effective potential is constructed from these dispersions. On the other hand, in Ref. [6], the coupled gap equation is exactly solved with non-perturbative treatment of M_s. However, one must say that their construction of the effective potential is quite ambiguous and, as we shall show, maybe possibly fails because of the multiplicity of the gap parameter. Even though their results are in good accordance with each other, there still exist a possibility that they missed the true solution. Furthermore, we have no strong universality argument that the unlocking transition must be of 1st order one, because the $SU(3)_V$ is already fallen into the $SU(2)_V$ isospin symmetry in the presence of finite strange quark mass.

In the present paper, we study the unlocking transition in more complete way than the

past work, by making a proper use of the Pauli construction of complete effective potential [1]. In particular, we study how the CFL state and other states are realized in the multi-gap parameter space and how the potential surface gets distorted with increasing the value of M_s^2/μ. Throughout this paper, we ignore the bulk neutrality conditions and treat the strange quark mass M_s as a parameter and draw phase diagrams in (Δ, T, M_s) parameter space, leaving more complete self-consistent analyses in future problems. In addition, we pay a special attention to the strange quark density as a function of M_s, to explore the possibility of Bose-Einstein condensation (BEC) of the tightly bound pairs in the low strange quark density regime. The crossover from the weak coupling BCS state to the strong coupling BEC state with decreasing density (increasing M_s at fixed μ), or increasing coupling, is a universal phenomenon in non-relativistic systems, such as in the electronic superconductor [13], in the general fermion system interacting via 2-body attractive force [14], in the nuclear matter with (p,n) pairing [15], and is also suggested in relativistic systems, including the 2SC phase [16] and in two-color QCD [17]. The characteristic feature of this crossover phenomenon shows up in the relation between chemical potential μ and density n, it is interesting to examine this possibility in our case of relativistic quark matter with the strong pairing interaction.

This paper is organized as follows. In Sec. II, we introduce our model, and present a general framework to obtain the gap equation and the effective potential, taking special care of the multiplicity of the gap parameter. Sec. III is devoted to the numerical analyses on the gaps, effective potential, and strange quark density varying the strange quark mass and temperature of the system. A novel aspect of the unlocking transition manifests itself, and its physical interpretation is also proposed. The phase structure in (T, μ, M_s) parameter space in our model is unveiled. In Sec. IV, we make summary and concluding remarks of this work.

II. FORMULATION

In this section, we present an outline for obtaining the gap equations and the effective potential with which we can determine the ground state of the system characterized by (Δ, T, M_s) parameter. We give a framework to derive the gap equation, which is applicable

[1] This procedure generates a non-trivial quadratic mean field term in the effective potential. The author thanks T. Kunihiro for pointing its importance out.

even for the more general case with the non-local interaction than with point-like interaction, until we specify the detail of our model in Sec. IIB.

A. Gap equations

Gap equation can be constructed by the self-consistency condition for 1PI (proper) self-energy. We specify the model space by color, flavor and spinor structure of the self-energy. As for the spinor structure, we consider the case of $J^P = 0^+$ channel only, and which is guaranteed by γ_5 in the self-energy matrix.

Self energies. We first introduce the color-flavor mixed quark base: $q = \sum_{a,i} q^{a,i} (\lambda^A/\sqrt{2})^i_a q^a_i$; where A ($A = 1 \cdots 8$) are the Gell-Mann matrices and we defined $(\lambda^9)^a_i = \sqrt{\frac{2}{3}}\,\delta^a_i$. Then the Nambu-Gor'kov propagator in the 2-compnent quark field $Q = (q, q^t)$ is written as

$$S(q_0,\mathbf{q}) \equiv -i\langle T\{Q(x)\bar{Q}(0)\}\rangle = \begin{pmatrix} \not{q} + \not{\mu} - M & \Delta(q_0,\mathbf{q}) \\ \Delta(q_0,\mathbf{q})^\dagger & \not{q}^t + \not{\mu}^t + M \end{pmatrix}^{-1}. \tag{1}$$

$\Delta(q_0,\mathbf{q})$ is off-diagonal self-energy which gives rise to gaps in the quasi-quark dispersion. M is the quark mass matrix in the color-flavor mixed base:

$$M = \begin{pmatrix} 0 & 0_3 & & \\ & \frac{M_s}{2}(1_2 + \tau_2) & & \\ & & \frac{M_s}{2}(1_2 + \tau_2) & \\ & & & \frac{2M_s}{3} \\ & & & \frac{\sqrt{2}M_s}{3} \end{pmatrix} \quad \begin{matrix} \\ \\ \\ \frac{\sqrt{2}M_s}{3} \\ \frac{M_s}{3} \end{matrix}. \tag{2}$$

Here, $\tau = (\tau_1, \tau_2, \tau_3)$ are the Pauli matrices. The pure CFL ansatz for the off-diagonal self-energy is expressed in the color-flavor mixed base as following,

$$\Delta^{\rm CFL}(q_0,\mathbf{q}) = C\gamma_5 \begin{pmatrix} & & \Delta_8 1_8 \\ & & \\ & \Delta_1 & \end{pmatrix}. \tag{3}$$

Here, C is the charge conjugation matrix $C = i\tau_2\gamma_0$. On the other hand, we would have the 2SC state with u-d pairing $\Delta^{\rm 2SC_{ud}} = \Delta_{ij}{}^{ab3}$ $\Delta^{\rm 2SC} = \Delta_A\,\delta_{ij}{}^{ab3}$ for sufficiently large value of M_s, which is written as

$$\Delta^{\rm 2SC_{ud}}(q_0,\mathbf{q}) = C\gamma_5 \begin{pmatrix} & \Delta_{\rm 2SC} 1_3 & & \\ & & 0_4 & \\ & & & \frac{1}{3}\Delta_{\rm 2SC} \\ & & & \frac{\sqrt{2}}{3}\Delta_{\rm 2SC} \end{pmatrix} \quad \begin{matrix} \\ \\ \\ \frac{\sqrt{2}}{3}\Delta_{\rm 2SC} \\ \frac{2}{3}\Delta_{\rm 2SC} \end{matrix}; \tag{4}$$

in the color- avor mixed base. As we shall derive later, the gap equation for this 2SC state does not depend on the value of M_s. From the two expressions for the 2SC and CFL phases, it is quite natural to expect the distorted CFL state (dCFL), the minimal interpolating pairing ansatz between those phases, for the small but nite strange quark mass [5, 6],

$$ {}^{dCFL}(q_0;q) \overset{M_s<M_s^c}{=} C_5 \begin{pmatrix} {}_{83}1_3 & & & \\ & {}_{82}1_4 & & \\ & & {}_{81} & \\ & & & {}_{11} \end{pmatrix} : \tag{5} $$

In this parameterization, the $SU(3)_{C+V}$ symmetric CFL phase and $SU(2)_C$ $SU(2)_F$ symmetric 2SC phase are expressed only as di erent limits of the dCFL phase which is invariant under color avor simultaneous rotation $SU(2)_{C+V}$. We introduce the 5-dimensional vector $\tilde{} = ({}_{83}; {}_{82}; {}_{81}; ; {}_{11})^t$. Using this notation, the model space for the pure CFL state can be expressed by the gap parameter $\tilde{}_{CFL} = ({}_8; {}_8; {}_8; 0; {}_1)^t$, which spans a 2-parameter section of the full model space. On the other hand, the 2SC phase is characterized by the 1-parameter vector $\tilde{}_{2SC} = ({}_{2SC}; 0; {}_{2SC}=3; \sqrt{2}\, {}_{2SC}=3; 2 {}_{2SC}=3)^t$.

Propagators. The anomalous propagator is de ned by the o -diagonal element of the Nambu-Gor'kov propagator,

$$ hT\, q\ (x)q\ (y)i = i \int \frac{d^4q}{(2\ )^4} e^{\ iq(x\ y)} S_{12}\ (q); \tag{6} $$

where S_{12} takes the following form for our ansatz Eq. (5),

$$ S_{12}\ (q) = {}_5C \begin{pmatrix} R_{83}1_3 & & & \\ & R_{82}1_4 & & \\ & & R_{81} & R \\ & & R & R_{11} \end{pmatrix} : \tag{7} $$

Here, $R_{81}({}_{81}; ; {}_{11})$, $R({}_{81}; ; {}_{11})$ and $R_{11}({}_{81}; ; {}_{11})$ are complicated functions of $(\tilde{}; ; M_s)$, some of which we summarize in the appendix.

Gap equations. The gap equation (the Schwinger-Dyson equation) is obtained by using Feynman rule for the self consistency between proposed self-energy and the one-loop self-energy.

$$ i \quad (p) = \int \frac{d^4q}{(2\ )^4} (\ ig(\ ^t)\ (T^a)^t\ )iS\ \ (q)(ig\ \ (T^a)\ \ )iD\ \ (q\ \ p): \tag{8} $$

The bare vertex in the color- avor mixed base is de ned by (T^a) $= \mathrm{tr}[\ _a\ ]/4$. D $(q$ $p)$ is the gluon propagator. By putting D $(q$ $p) \to$ g, we arrive at the gap equation for the NJL model with the vertex for one-gluon exchange $L_{int} = (1/2)g^2 q\ t^a q q\ t^a q$,

$$= i4g^2 \int \frac{d^4q}{(2\ )^4} (T^a)\ \ S\ \ (q)(T^a)\ \ : \tag{9}$$

This integral matrix equation contains the following set of ve equations.

$$_{83} = g^2 \frac{1}{12}\ \ 5R_{\ 83}\ \ R_{81}\ \ 2\sqrt{2}R\ \ \ 2R_{11}\ \ ; \tag{10}$$

$$_{82} = g^2 \frac{1}{12}\ \ 2R_{\ 82} + 2R_{\ 81} + \sqrt{2}R\ \ \ 2R_{11}\ \ ; \tag{11}$$

$$_{81} = g^2 \frac{1}{12}\ \ \ 3R_{83} + 8R_{\ 82}\ \ \ R_{81} + 2\sqrt{2}R\ \ \ 2R_{11}\ \ ; \tag{12}$$

$$= g^2 \frac{\sqrt{2}}{12}\ \ \ 3R_{83} + 2R_{\ 82} + R_{\ 81}\ \ \ \sqrt{2}R\ \ ; \tag{13}$$

$$_{11} = g^2 \frac{1}{6}\ \ \ 3R_{83}\ \ \ 4R_{82}\ \ \ R_{81}\ \ : \tag{14}$$

Here, we have de ned R by

$$R_{\ i}(\tilde{\ };M_{\ s}) = i \int \frac{d^4q}{(2\ )^4} \frac{1}{4} \mathrm{tr}\left[C\ _5 R_{\ i}(q;\tilde{\ };M_{\ s}) \right] : \tag{15}$$

conversely, the Eqs. (10) (14) can be inverted into the following set of the equations by solving $fR_{\ 83}; R_{\ 82}; R_{\ 81}; R\ ; R_{\ 11}g$ formally as a function of the gap parameters $\tilde{\ }$,

$$\frac{3}{8g^2}\ \ \ _{83}\ \ \ _{81}\ \ \sqrt{2}\ \ \sqrt{2}\ \ \ 2\ \ _{11}\ \ = R_{\ 83}(\tilde{\ };M_{\ s}); \tag{16}$$

$$\frac{3}{8g^2}\ \ \ 2\ _{82} + 2\ _{81} + \sqrt{2}\ \ \ 2\ \ _{11}\ \ = R_{\ 82}(\tilde{\ };M_{\ s}); \tag{17}$$

$$\frac{3}{8g^2}\ \ \ 3\ _{83} + 8\ _2\ \ \ 5\ _{81} + 2\sqrt{2}\ \ \ 2\ \ _{11}\ \ = R_{\ 81}(\tilde{\ };M_{\ s}); \tag{18}$$

$$\frac{3\sqrt{2}}{8g^2}\ \ 3\ _{83}\ \ \ 2\ _{82}\ \ \ _{81} + 3\sqrt{2}\ \ \ = R\ (\tilde{\ };M_{\ s}); \tag{19}$$

$$\frac{3}{4g^2}(3\ _{83} + 4\ _{82} + 2\ _{81} + 2\ _{11}) = R_{\ 11}(\tilde{\ };M_{\ s}): \tag{20}$$

We should show in the next section that each of these equations is nothing but the derivative of the e ective potential in terms of corresponding gap parameter.

Quark density. The quark density is related to the diagonal (1,1) element of the Nambu–Gor'kov propagator (see Eq. (1)),

$$hT\, q\ (x)q\ (y)i = i \int \frac{d^4q}{(2\ )^4} e^{\ iq(x\ \ y)} S_{11}\ (q): \tag{21}$$

S_{11} takes the following matrix form for the our model space of the order parameter,

$$S_{11} = \begin{pmatrix} T_{83}1_3 & & & & \\ & T_{82}1_2 + T_{82}{}_2 & & & \\ & & T_{82}1_2 + T_{82}{}_2 & & \\ & & & T_{81} & T \\ & & & T & T_{11} \end{pmatrix} : \tag{22}$$

Total quark density can be extracted from the propagators as

$$= \sum_{i=1}^{9} i \int_{C_+} \frac{d^4q}{(2\ )^4} \mathrm{tr}[\ {}_0S_{11}\ (q;\ ;M\ {}_s)] = 3\ {}_{83} + 4\ {}_{82} +\ {}_{81} +\ {}_{11} : \tag{23}$$

Here we have defined

$${}_i[\ ;M\ {}_s] = \int_{C_+} i \frac{d^4q}{(2\ )^4} \mathrm{tr}[I_i(q;\ ;M\ {}_s)]; \tag{24}$$

and C_+ represents the integral along the contour enclosing anticlockwise the upper half q_0-plane. Similarly, the strange quark density is obtained as

$${}_s = \frac{2}{3}\ {}_{81} + \frac{1}{3}\ {}_{11} \quad \frac{2^p\overline{2}}{3}\ + 2\ {}_{82} \quad 2\ {}_{82} : \tag{25}$$

B. Effective potential for multi-gap parameters

In this section, we specify our model in detail in order to obtain the expression of the effective potential by applying the Pauli construction. We start from the NJL Hamiltonian density in the color-flavor mixed base:

$$H \quad N = q^+ f(i\tilde{} \quad r \quad) + M \quad {}_0gq + H_{int:}; \tag{26}$$

with the interaction with one-gluon exchange vertex:

$$H_{int:} \quad \frac{1}{2}g^2 \sum_{a=1}^{8} (q\ (T^a) \quad q\ )(q\ (T^a) \quad q\ ): \tag{27}$$

Here we have defined $\tilde{} \quad {}_0\tilde{}$. The mean field approximation (MFA) can be made by putting the CFL-2SC interpolating ansatz for $hqqi$ correlation,

$$hq_i\ q_j i = (C\ {}_5)_{ij} \quad ; \quad hq_i\ q_j i = \quad ({}_5C)_{ij}\ {}^+ \quad : \tag{28}$$

The Greek character $(i; j;\ )$ should be regarded as spinor indices. We define the quantities having the dimension of energy as

$$= 4g^2 (T^a)\qquad (T^a)\ : \tag{29}$$

$f\ _i g$ can be determined uniquely by $f\ _i g$. The MFA is made through the procedure:

$$2H_{\text{int:}} \overset{M,FA}{!} (q_i q_k)\qquad (\ _5C)_{ik} + (h:c:) + 4tr_{CF}\ ^{+}\ : \tag{30}$$

If we assume the CFL-2SC interpolating ansatz for the condensate matrix form of and the gap parameter matrix as

$$= \begin{pmatrix} 0 & & & \\ & {}_{83}1_3 & & \\ & & {}_{82}1_4 & \\ & & & {}_{81} \end{pmatrix}; \qquad = \begin{pmatrix} 0 & & & \\ & {}_{83}1_3 & & \\ & & {}_{82}1_4 & \\ & & & {}_{81} \end{pmatrix}: \tag{31}$$

$\tilde{} = (\ _{83};\ _{82};\ _{81};\ ;\ _{11})^t$ and $\tilde{} = (\ _{83};\ _{82};\ _{81};\ ;\ _{11})^t$ are related by Eq. (29), which leads to

$$\tilde{} = \frac{3}{8g^2}\hat{A}\tilde{};\tag{32}$$

where the matrix $\hat{A}$ relating the condensates to the gap parameters is defined as

$$\hat{A} = \begin{pmatrix} 0 & 1 & 0 & 1 & \frac{p}{2}\overline{2} & 2^1 \\ 1 & 0 & 2 & 2 & \frac{p}{2}\overline{2} & 2 \\ 3 & 8 & 5 & \frac{p}{2}\overline{2} & 2 & \\ \frac{p}{3}\overline{2} & 2\frac{p}{2}\overline{2} & \frac{p}{2}\overline{2} & 6 & 0 & \\ 6 & 8 & 2 & 0 & 4 & \end{pmatrix}: \tag{33}$$

Using this matrix $\hat{A}$, the gap equations derived in the previous section can be expressed simply as

$$\tilde{} = \frac{3}{8g^2}\hat{A}\tilde{}\qquad \tilde{R}\,[\tilde{};M_{\ s}];\tag{34}$$

with the definition $\tilde{R} = (R_{\ 83}; R_{\ 82}; R_{\ 81}; R_{\ }; R_{\ 11})$, where the kernels $fR_{\ i}g$ are defined by Eq. (15).

Pauli construction of the effective potential. We use the Pauli trick [2] to derive Effective

[2] The author is thankful to T. Kunihiro who suggested me to use this method to construct the effective potential taking care of the multiplicity of the gap parameter.

potential with help of the gap equations.

$$\frac{}{g^2} = \frac{1}{g^2}\langle H_{int}\rangle = \quad \frac{3}{4g^4}(\tilde{\ }; \hat{B}\hat{A}\tilde{\ }): \tag{35}$$

Here $\hat{B}$ is degeneracy matrix $\hat{B} = \mathrm{diag}:(3;4;1;2;1)$, and $(\ ;\ )$ represents the inner product defined in 5-gap parameter space as $(A;B) \quad \sum_{i=1}^{5} A_i B_i$. Note that $\hat{B}\hat{A}$ is a real-valued symmetric matrix. By integrating over the variable g^2 from 0 to g^2, we obtain the effective potential relative to the naive Fermi gas of 2 massless (u;d) quarks and strange quark with mass M_s, namely, $_e[\ ;\tilde{\ };M_s] \quad [\ ;\tilde{\ };M_s] \quad {}_0^{2+1}[\ ;M_s]$,

$$\begin{aligned}
{}_e[\ ;\tilde{\ };M_s] &= \int_0^{g^2} dg^2 \ \frac{3}{4g^4}(\tilde{\ }; \hat{B}\hat{A}\tilde{\ }) \\
&= \frac{3}{4g^2}(\tilde{\ }; \hat{B}\hat{A}\tilde{\ }) \quad \int_0^{g^2} dg^2 \ \frac{\tilde{\ }}{g^2}; \frac{3}{2g^2}\hat{B}\hat{A}\tilde{\ } \\
&= \frac{3}{4g^2}(\tilde{\ }; \hat{B}\hat{A}\tilde{\ }) \quad 4\int_0^{\tilde{\ }} \tilde{\ }; \hat{B}\tilde{R}[\tilde{\ };M_s] :
\end{aligned} \tag{36}$$

Here, we have defined $\tilde{\ } = (_{83};\ _{82};\ _{81};\ ;\ _{11})^t$. Second line to third line, we have used the gap equation

$$\hat{A}\tilde{\ } = \ \frac{8}{3}g^2\tilde{R}[\tilde{\ };M_s]; \tag{37}$$

with the degeneracy matrix $\hat{B} = \mathrm{diag}:(3;4;1;2;1)$. Also the one to one correspondence between g^2 and $\tilde{\ }$ is assumed. Eq. (36) is a formula of the effective potential, when the kernel of the gap equation is already known. The second term in Eq. (36) represents the condensation energy. We can easily check the fact that the first derivative of the effective potential is equivalent with the gap equation:

$$\hat{B}^{\ 1}\frac{}{\tilde{\ }} = \frac{3}{2g^2}\hat{A}\tilde{\ } \quad 4\tilde{R}[\tilde{\ }] = 0: \tag{38}$$

What should be stressed here is that the derivative of the effective potential is not exactly of the same form as the original gap equations set Eqs. (10) (14), but coincides with some linear combinations of those, namely, Eqs. (16) (20). This means that we might miss the true effective potential if we construct it from the integral of the original kernel in Eqs. (10) (14). The second term in Eq. (36) corresponding to condensation energy is hard to evaluate the gap-integral except for the iso-triplet and iso-doublet blocks, namely, the integral containing R_{83} and R_{82}. Thus we shall try to evaluate these numerically. However,

there are two cases in which the effective potential can be written in simple forms, which we summarize in the appendix.

Grand potential. The effective potential Eq. (36) reduces to the following form when is evaluated at the solution $\tilde{}_{sol} = (g; ; M_s)$ of the gap equation Eq. (34)

$$_{cond.}(; M_s) \quad _e [; \tilde{}_{sol}; M_s] = 2(\tilde{}_{sol}; \hat{B}\tilde{R}[\tilde{}_{sol}; M_s]) \quad 4 \int_0^{\tilde{}_{sol}} \tilde{}; \hat{B}\tilde{R}[\tilde{}; M_s] : \quad (39)$$

This is the (thermodynamic) grand potential relative to the naive Fermi gas with (u;d;s). This quantity depends on (;T;M_s), and its derivative in terms of (;T) is nothing but ($_{rel}$;S_{rel}), namely, the quark density and the entropy relative to the simple Fermi gas. This formula Eq. (39) is useful because the coupling g^2 does not enters this formula explicitly, but does implicitly through the gap $\tilde{}_{sol}$.

III. NUMERICAL RESULTS

Here, we present our numerical results. The cutoff parameter is set to = 800MeV, and the coupling parameter g^2 is tuned to reproduce 400MeV for the constituent mass of quark at zero chemical potential [6]. We have checked all of the main results here are robust against the variation of the cutoff parameter.

A. Solution of gap equation

We shall display the solution of the coupled gap equation Eqs. (16) (20) as a function of strange quark mass M_s. The parameters (b;c;d;e;f) are defined by the gap parameters ($_{83}$; $_{82}$; $_{81}$; ; $_{11}$) via the following one to one linear relation:

$$\begin{pmatrix} b \\ c \\ d \\ e \\ f \end{pmatrix} = \begin{pmatrix} 1 & 0 & 1=2 & 0 & 1=6 & p\overline{2=3} & 1=3 \\ 0 & 0 & 1=3 & 0 & p\overline{2=6} & 1=3 & 0 \\ 0 & 0 & 2=3 & 0 & p\overline{2\ 2=3} & 1=3 & 0 \\ 1 & 0 & 0 & 0 & 0 & 0 & 1 \\ 0 & 1 & 0 & 0 & 0 & 0 & \end{pmatrix} \begin{pmatrix} {}_{83} \\ {}_{82} \\ {}_{81} \\ \\ {}_{11} \end{pmatrix} : \quad (40)$$

This is equivalent with the parameterization introduced by Berges et al [6]. In this base, the CFL state is characterized by (c = b;f = e;d = b+ e 6 0) and the 2SC state is expressed by (b = e;c = d = f = 0). Our gaps show almost the same behavior as in the ref. [6] for

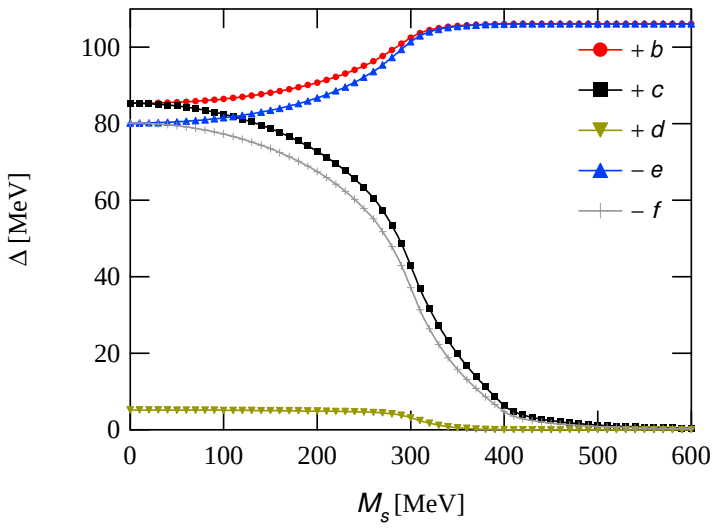

FIG. 1: The gaps as a function of strange quark mass M_s at $\mu = 400$MeV, and $T = 0$. The fermionic mass spectral in the CFL state at $M_s = 0$ seems continuously connected to those in the 2SC state.

$M_s \lesssim 250$ MeV. However, the difference comes out for $M_s \gtrsim 250$ MeV at which the CFL state is supposed to get unlocked to the 2SC state by 1st order transition [6]. In our case, the system goes continuously from the CFL to the 2SC state, though it is not clear whether the transition is 2nd order one, or higher order, or the smooth cross over. We will see later that even in our case, the 2SC is always a solution of the gap equation, but actually with higher energy than the CFL state. In FIG. 2(a), we show the eigenvalues of the original gap matrix Eq. (5) as functions of M_s. $(\Delta_{83}, \Delta_{82})$ are the gaps for iso-triplet and doublet fermionic excitations. (Δ_1, Δ_2) are the eigenvalues of the iso-singlet mixed sector,

$$\Delta_{1(2)} = \frac{1}{2}\left(\Delta_{81} + \Delta_{11}\right) \mp \sqrt{\left(\Delta_{81} - \Delta_{11}\right)^2 + 4\Delta^2}\,. \tag{41}$$

In the pure CFL state, $(\Delta_1, \Delta_2) = (\Delta_1, \Delta_8)$, and in the 2SC state, $(\Delta_1, \Delta_2) = (\Delta_{2SC}, 0)$. However, we note that in the distorted CFL state for moderate M_s, the true gaps for the fermionic excitation is defined by more complicated functions of $(\mu, M_s, \Delta_{81}, \mu, \Delta_{11}, M_s)$, which are the minimums of two dispersion $z_{1,2}(p, \mu, \Delta_{81}, \mu, \Delta_{11}, M_s)$, namely, the solutions of the quartic algebraic equation which we give explicitly in Eq. (A4). According to the values of these parameters, the states are distinguished by

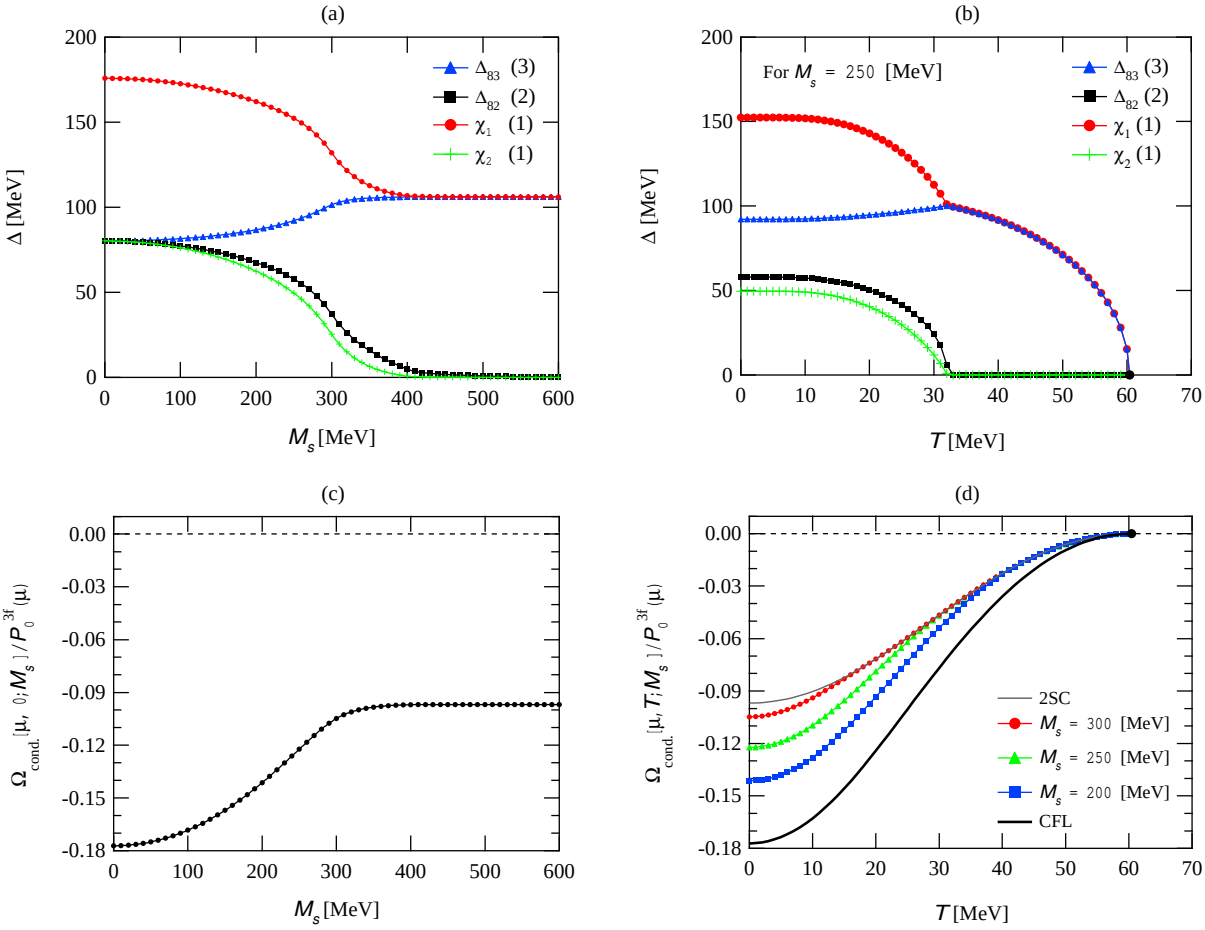

FIG. 2: (a) Gaps are plotted as functions of M_s. (b) The temperature dependence of the gaps for $M_s = 250$ MeV. (c) The grand potential of the pairing state relative to the non-interacting Fermi gas with (u;d;s) quarks is plotted as a function of M_s. (d) The grand potential as a function of T for $M_s = 0$ (the CFL state), $M_s = 200;250;300$ MeV and for M_s (the 2SC state).

Gap parameters	Symmetry	States
$_{83} = _{82} = _2; _1 \neq 0$	$SU(3)_V$	CFL for $M_s = 0$
$_{83} = _1; _{82} = _2 = 0$	$SU(2)_F$ $SU(3)_c$	2SC for $M_s > M_s^c$
otherwise	$SU(2)_V$	distorted CFL (dCFL)

It is surprising that the system stays in the distorted CFL (dCFL) phase even for $M_s \& = 400$ MeV. In FIG. 2(b), we display the gaps ($_{83}$; $_{82}$; $_1$; $_2$) for $M_s = 250$ MeV as functions of temperature. We see that as the temperature is raised, the dCFL phase encounters the continuous transition to the 2SC state at $T = 35$ MeV, and eventually the system undergoes 2nd order phase transition to the normal fermi-liquid at $T = 60$ MeV.

In order to see aspects of the phase transition to the 2SC state with increasing M_s or T in more detail, we study the bulk quantities as well as the gaps. In FIG. 2(c), we show the grand potential relative to the non-interacting gas with two massless (u,d) quarks and s quark with mass M_s, namely, $\Omega_{\rm cond.}(\mu, M_s) = \Omega(\mu, M_s) - \Omega_0^{2+1}(\mu, M_s)$ (see Eq. (39)) in the unit of the pressure of the massless 3 flavor normal Fermi gas $P_0^{3f}(\mu) = 3\mu^4/4\pi^2$. In the chiral limit, the system is in the pure CFL state. As increasing the strange quark mass M_s, the grand potential gradually decreased, and saturates to the value for the 2SC state. The condensation energy for the pure CFL state is almost 1.9 times as large as that for the 2SC state, which is consistent with the weak coupling analysis [18] and also with Schwinger-Dyson approach [19]. From this figure, it is not still clear whether the unlocking transition at $T = 0$ is of continuous 2nd order or higher order, or even the smooth crossover. In FIG. 2(d), $\Omega_{\rm cond.}(\mu, T, M_s)/P_0^{3f}(\mu)$ is plotted as a function of T, for strange quark masses $M_s = 0$ (pure CFL); 200; 250; 300; ∞ (2SC). The critical temperatures of the transition to normal fermi gas are all the same ($T_c = 60$ MeV) for all values of the strange quark mass [19]. The grand potential for all values of M_s approaches the 2SC curve towards some temperature $T_c^{\rm unlock}(M_s) < T_c$, at which the continuous unlocking transition occurs. This unlocking critical temperature $T_c^{\rm unlock}(M_s)$ is the decreasing function of M_s. This is because the energy gain of the CFL state relative to the 2SC state gets smaller with increasing M_s, as is clear from FIG. 2(c). We discuss the $(M_s; T_c^{\rm unlock})$ relation in more detail later.

B. Effective potential for multi-gap parameter space

In the previous section, we saw that the CFL state is always stable relative to the 2SC state for $M_s < \infty$ by analyzing the grand potential. Now, by computing the effective potential with help of the formula Eq. (36), we study how these states are realized in the multi-gap parameter space. There is still a possibility that these states are just saddle points of the effective potential. In FIG. 3, we display the effective potential $\Omega_{\rm eff}[\tilde{\Delta}; M_s]$ in the section spanned by the 2SC gap $\tilde{\Delta}_{\rm 2SC} = (106; 0; 35; 50; 70)$ MeV and the CFL gap $\tilde{\Delta}_{\rm CFL} = (80; 80; 80; 80; 175)$ MeV. By introducing the vector $\tilde{\Delta}(i,j) = \frac{(i-10)\tilde{\Delta}_{\rm CFL} + (j-10)\tilde{\Delta}_{\rm 2SC}}{50}$, we define 2-dimensional planer section in the 5-dimensional gap parameter space, which includes the simple Fermi gas (10,10) with $\tilde{\Delta} = 0$, the CFL (60,10) and the 2SC (10,60). In FIG. 3, the values of the effective potential $\Omega_{\rm eff}[\tilde{\Delta}(i,j)]$ are contoured as a function of (i,j)

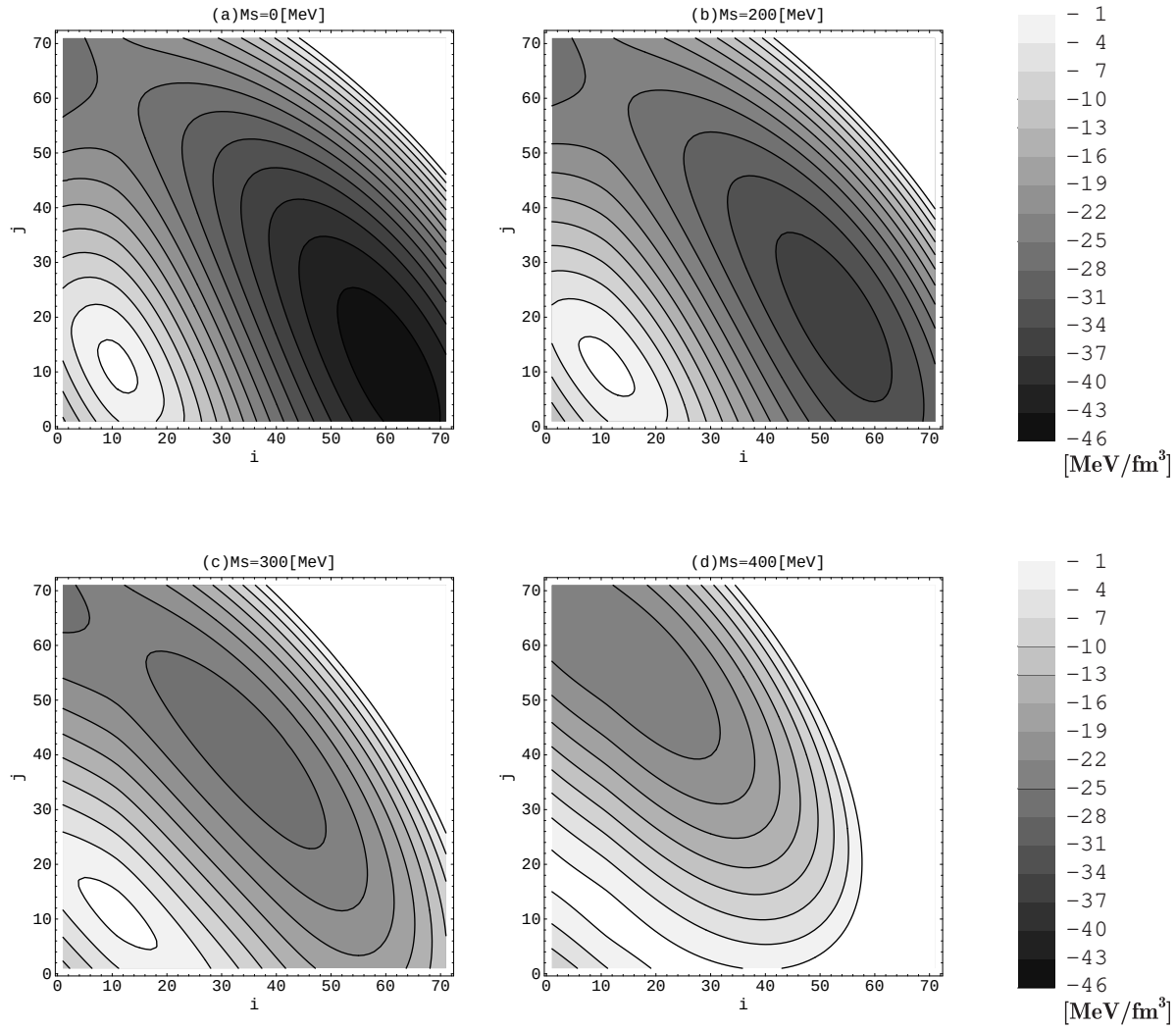

FIG. 3: Contour plot of the effective potential for $(T, \mu) = (0, 400)$ MeV in the 2-dimensional sector spaned by the CFL gap vector $\tilde{\Delta}_{CFL} = (80, 80, 80, 175)$ MeV and the 2SC gap vector $\tilde{\Delta}_{2SC} = (106, 0, 35, 50, 70)$ MeV. Effective potential surface for $M_s = 0$ MeV (a), $M_s = 200$ MeV (b), $M_s = 300$ MeV (c), and for $M_s = 400$ MeV (d). In figure, the point $(i, j) = (10, 10)$ corresponds to the normal fermi gas with 2 massless flavor and 1 massive strange quark. The points (60, 10) and (10, 60) corresponds to the pure CFL state and the 2SC state, respectively.

for $M_s = 0$ MeV (a), 200 MeV (b), 300 MeV (c) and 400 MeV (d). We can see that the CFL state (60, 10) looks the global minimum in this 2-parameter space (i, j) for $M_s = 0$ MeV. On the other hand, the 2SC state (10, 60) is realized as a saddle point which is stable in the direction of the simple Fermi gas (10, 10), but is unstable in the direction towards the CFL

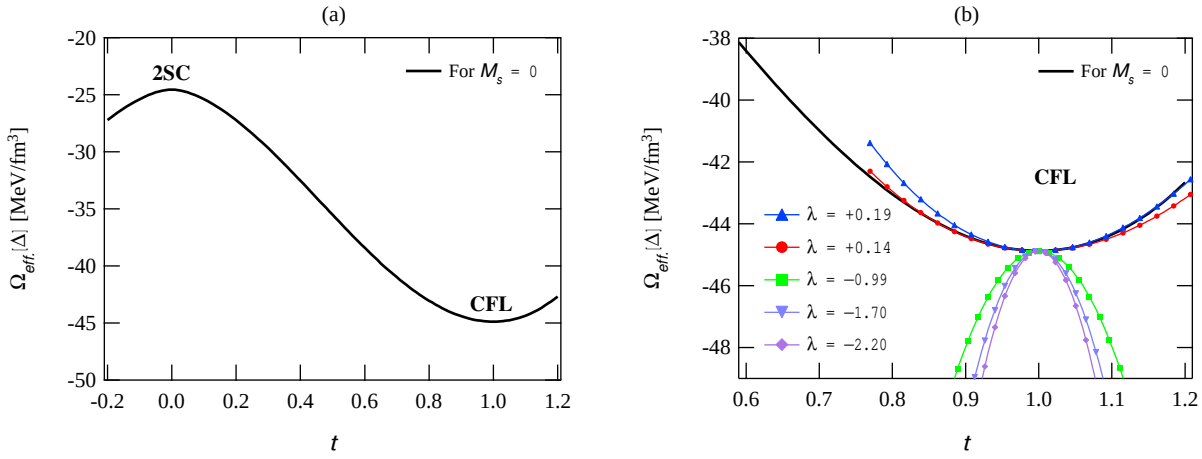

FIG. 4: (a) The values of the effective potential on the 1-dimensional line connecting from the 2SC state $t = 0$ to the CFL state $t = 1$. (b) The bold line is just an enlargement of the potential curve for $M_s = 0$ in (a), and five set of the points (triangles, bold dots, squares, reflected triangles, lozenges) represent the potential curves in the directions of the eigenvectors belonging to the five eigenvalues $= (0.19; 0.14; -0.99; -1.70; -2.20)^3$ of the Hessian curvature matrix at the CFL.

state $(60;10)$. As the strange quark mass is increased to 200 MeV, the CFL minimum moves towards the 2SC point, and its condensation energy gets reduced, while the position and the energy of the 2SC state is unaffected by M_s. This minimum point $(55;20)$ corresponds to the distorted CFL state [3]. The dCFL state gets distorted significantly towards the 2SC state at $M_s = 300$ MeV (FIG. 3(c)), and seems absorbed into the 2SC as the strange quark mass approaches the order of the chemical potential μ of the system. We can conclude that the unlocking transition is not of 1st order.

2SC as a solution of gap equation. What should be stressed here is that the 2SC stays at least a saddle point in the full model space irrespective of the value of M_s. This means that the 2SC is always a solution of the gap equation, and if we had missed in obtaining the correct effective potential, then we misunderstood it as the true ground state instead of the

[3] Strictly speaking, it is not necessary that this point does exactly coincide with the true dCFL point, because we restrict ourselves to drawing the effective potential even in the 2-dimensional planer in the 5-parameter space. But it is sufficient here to mention that the dCFL state other than the 2SC state exists near the point $(55;20)$ in full model space, and indeed, it has a larger condensation energy than the 2SC state.

dCFL state for intermediate strange quark mass M_s.

Unstable CFL vacuum. In FIG. 4(a), we plot the section of the effective potential surface FIG. 3(a) on the line linking the 2SC (10;60) $\tilde{}_{t=0} = \tilde{}_{2SC}$ and the CFL (60;10) $\tilde{}_{t=1} = \tilde{}_{CFL}$. Both states are determined by solving the gap equation in 5-gap parameter space for $M_s = 0$ MeV. Now we address the question whether the CFL state is true global minimum even in the full model space or not. FIG. 4(b) shows us the answer for this question. Five potential curves are shown near the pure CFL for $M_s = 0$, each of which represents the potential curve in the direction of an eigenvector belonging to the corresponding eigenvalue of the Hessian curvature matrix at the CFL point:

$$\frac{@^2}{@\ _i @\ _j}_{\tilde{}=\tilde{}_{CFL}} = \frac{3}{2g^2}(\hat{B}\hat{A})_{ji} \quad 4\hat{B}_{jl}\frac{@R_l[\tilde{}]}{@\ _i}_{\tilde{}=\tilde{}_{CFL}} : \tag{42}$$

What is surprising is that the CFL state is not the global minimum in the full model space. It is unstable in three out of five directions. These three directions correspond to the color-flavor sextet channels in which the interaction acts repulsive, as we show explicitly this fact in the appendix. Also it should be noted that the color-flavor sextet gap parameters do not break any symmetry, thus are not the order parameter for the unlocking as is anticipated in their critical behaviour $(1 \quad T=T_c)^{3=2}$ near critical temperature T_c in the chiral limit [19]. Anyway, because the effective potential becomes unbound once the sextet condensations are included, it makes no physical sense to include symmetric mean fields contribution [4, 20, 21] in the ansatz for the gap matrix from the beginning.

C. Strange quark density : Bose-Einstein condensation

We saw that the critical strange quark mass M_s^c is much larger than the value $\sqrt{\ }_8$ predicted from the kinematical picture for the unlocking, which says that the unlocking is caused by the balance between the mismatch of the Fermi momenta, and the magnitude of the gap. Indeed, the critical mass is located at $M_s \& \ $, and this fact suggest that our CFL state is much robuster than others obtained by several authors [5, 6]. We want to draw here a physical picture for our unlocking transition. We show how the strange quark density approaches zero with increasing the strange quark mass M_s in FIG. 5. The fine line is showing the quantity $_s^0 = {}^0 = \frac{1}{3}\ 1 \quad (M_s =)^{2\ 3=2}$; which is the ratio of the strange quark density $_s^0$ and the total density ^{0} in the unpairing matter. This quantity approaches

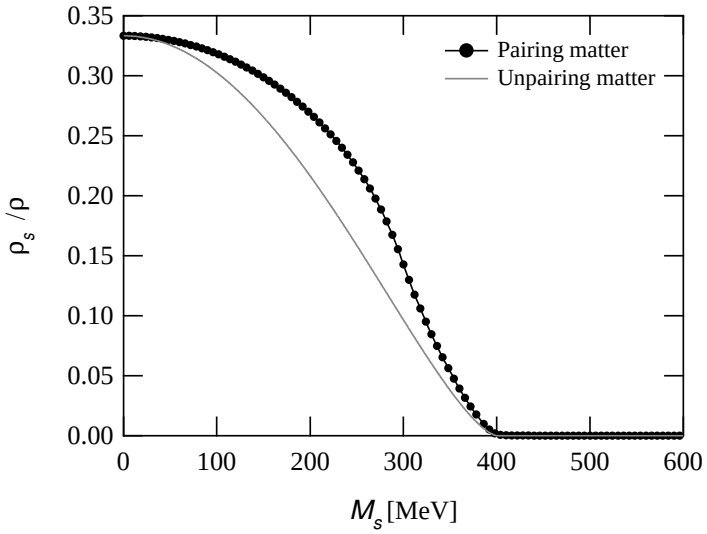

FIG. 5: The strange quark density $_s$ divided by the total quark number density as a function of M_s. The line shows the same quantity for the unpairing matter which consists of two massless (u;d) quarks and the strange quark with M_s.

zero with M_s ! very slowly, because its derivative in terms of M_s has no discontinuity at $M_s =$, but the third derivative has singular behavior $1=\sqrt{^2 \quad M_s^2}$ at the critical point. This means that the transition from the 2 + 1 matter to the 2 avor matter with increasing the strange quark mass is of 3rd order if the interaction does not exist. The bold dots represent the density fraction $_s=$ for the pairing matter (the CFL, dCFL, and 2SC states). It seems that this quantity falls to zero smoothly at M_s . FIG. 6 (a) is just an enlargement of FIG. 5 for the region $M_s = 550$ 750 MeV. Similarly, FIG. 6 (b) shows the iso-doublet gap $_{82}$ and the singlet gap $_2$ as functions of M_s for this region. Now we can see a clear signal for the phase transition from the dCFL phase to the 2SC state. The strange quark density becomes zero at $M_s^c = 680$ MeV, with the sadden fall of the gaps for modes containing strangeness. The unlocking phase transition from the CFL state to the 2SC state with increasing strange quark mass is clearly of 2nd order. The strange quark density intersects zero axis with a nite slope, which indicates that a derivative of the strange quark density with respect to M_s has a discontinuity at the critical mass M_s^c, namely the transition is of 2nd order. However, the strength of this 2nd order transition is very weak for $T = 0$ in the sense that the magnitude of the discontinuity in the M_s-derivative of strange quark density is very small. This discontinuity at the critical mass of the unlocking

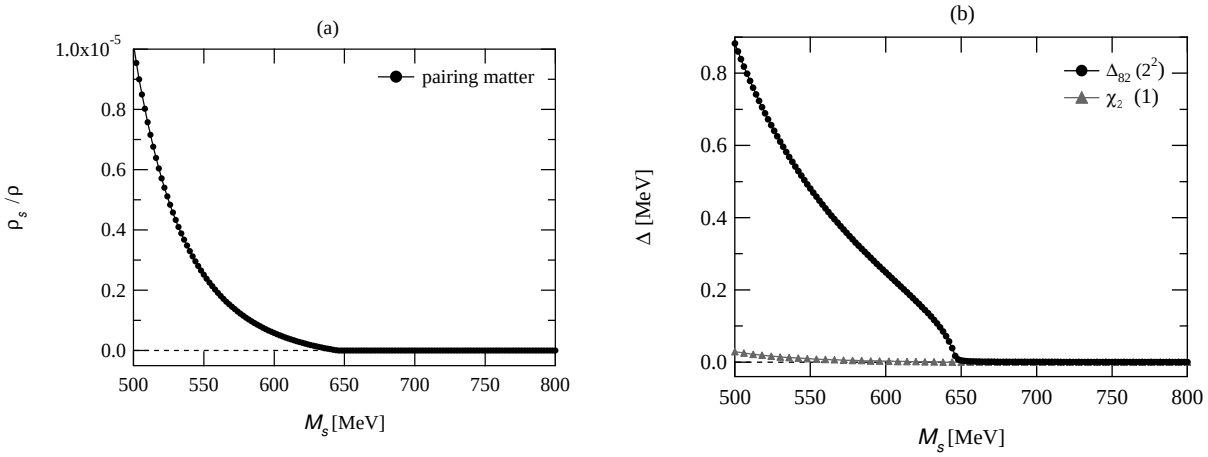

FIG. 6: (a) The enlargement of FIG. 5 for $M_s = 550 \quad 750$ MeV. (b) The gap for the iso-singlet excitation $_2$ and for the iso-doublet excitation $_{82}$ near the critical mass. This is just an enlargement of FIG. 2(a) for the same region of M_s as in (a).

transition becomes larger as we increase temperature of the system. In fact, we have a clearer kink in the fraction $_s=$ at the unlocking point at nite temperature, though $_s=$ does not get exact zero due to the Fermi-Dirac distribution at nite T.

We saw here that the unlocking occurs at a much larger mass M_s than the chemical potential . How we can understand this fact? We propose here the crossover from the BCS to the BEC at low strange quark density. In the non-relativistic electron system, or in the nuclear matter with (n;p) pairing, it is known that the BEC rather than BCS state realizes at low density or in the strong coupling regime [14, 15]. This crossover phenomenon with decreasing fermion density is signaled by the negative chemical potential < 0 at low density. The gap equation is the integral equation to determine the gap in the fermionic dispersion for a given chemical potential . This can be converted into the equation to determine the correlation function (k) and occupation number n(k) for a given , which reduces to the 2-body Schrodinger equation in the attractive potential in the low density limit $n(k) ! 0$, where the chemical potential plays a role of the energy eigenvalue. Thus the negative sign of the chemical potential for $! 0$ indicates the emergence of the bound state with binding energy $E_B = _{crit:}$. In the relativistic case, the situation is slightly different. The chemical potential does not approach zero but does the mass threshold with the density approaching zero in the case of free gas: $= \sqrt{(3^2=d)^{2=3} + M^2}$, where d is the degeneracy factor of the fermion. Thus, it is natural to speculate that if the CFL state melts to the 2SC state

at M_s^c (& 0) with the $_s = 0$, the BEC of the bound state which consists of light avors and strange quark with binding energy $E_B = M_s$ is realized for the low density region. In fact, we can show that the gap equation for the relativistic system reduces to the 2-body Klein-Gordon equation in the attractive potential in the limit $\to 0$. If this scenario is true, the binding energy at zero density is about $E_B = M_s^c$ can be of the order several hundreds MeV. If this is the case, we can expect the pair dissociation at higher temperature T_d than the critical temperature for Bose-Einstein condensation $T_{BEC} = \frac{2}{M_B}(= (3))^{3=2}$; where M_B is mass of the boson. In this case, the system in $T_{BEC} < T < T_d$ may be described by the thermal boson gas with no phase coherence, which may be relevant to so-called "pseudogap" phenomenon in the high T_c superconductor [22]. Also, the results obtained in Refs. [23, 24] suggest the existence of the bosonic collective modes above the critical temperature, where the symmetry is already recovered. Our BCS-BEC crossover scenario might provide another description of the pseudogap phenomenon. We would formulate the pseudogap phase based on this picture elsewhere by analysing the bound state equations for q-q pairs at nite temperature.

D. Phase diagrams

We here show two phase diagrams determined by constructing the e ective potential for multi-gap parameters. In FIG. 7, we show the phase diagram in $(T; M_s)$ plane. At $M_s = 0$, we have the CFL phase for $T < T_c$, and the normal fermi gas phase for $T > T_c$. Both phases are divided by 2nd order phase transition. As the strange quark mass is increased, we have three phases according to the region of temperature, the dCFL phase for low temperature $T < T_c^{unlock}$, the 2SC phase for $T_c^{unlock} < T < T_c$, and the normal Fermi gas of quarks for $T > T_c$. These three phases are divided by 2nd order phase transition. T_c^{unlock} is the deacreasing function as increasing strange quark mass, while T_c is una ected by the increase of M_s. The former results from the smaller condensation energy for dCFL state as increasing M_s, and the latter is attributed to the fact that the the parameter M_s is completely decoupled from the 2SC gap equation. $T_c^{unlock} = 35$ MeV at $M_s = 250$ MeV, which we saw exactly in FIG. 2(b). As we have discussed in the previous section, the dCFL phase exists for $M_s >$ where the BEC of tightly bound pairs constituted with strange quark and (u;d) quarks might be realized. Also, in this BEC region, we might have a pseudogap like phase of the

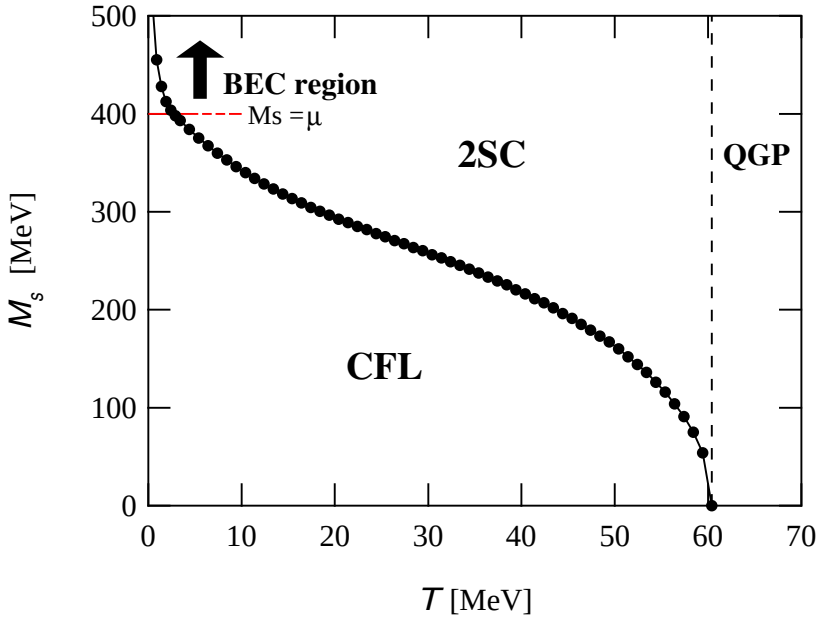

FIG. 7: Phase diagram in $(T; M_s)$ plane for $\mu = 400$ MeV. Bold dots represent the color-flavor unlocking line separating the superconducting area into the dCFL and 2SC phases, while the dashed line $T \simeq 60$ MeV is a phase boundary between the 2SC phase and the normal Fermi gas.

Bose gas without any phase coherence above the critical temperature $T_c^{\rm unlock}(M_s) < T < T_c$.

Finally, we show the phase diagrams in the entire $(\mu; T)$ plane in FIG. 8. FIG. 8(a) shows the phase diagram for $M_s = 400$ MeV. The squares represent the color-flavor unlocking line on which the CFL (2SC) state turns into the 2SC (CFL) phase. We can see clearly that our CFL phase are much robuster than that obtained through the kinematical criterion which says, if the strange quark mass is increased so that the mismatch of Fermi momenta of two species exceed the value:

$$\sqrt{\mu^2 - M_s^2} = \frac{M_s^2}{2\mu} \simeq 2|\Delta_8(T)|_{M_s=0};$$

then the CFL gets unlocked to the 2SC phase by 1st order phase transition. The order of the phase transition is 2nd order as we discussed, which also contradicts the simple kinematical picture for the unlocking. The region $\mu \simeq M_s = 400$ MeV, we still have a slight region for dCFL phase at $T < T_c^{\rm unlock}(M_s = 400; \mu) \simeq T_c$. In this region, we expect the BEC like state with tightly bound pairs of strange and light flavors, and above this phase we might have a possible pseudogap phase of thermal Bose gas.

In FIG. 8(b), we show the unlocking line and its dependence upon the strange quark

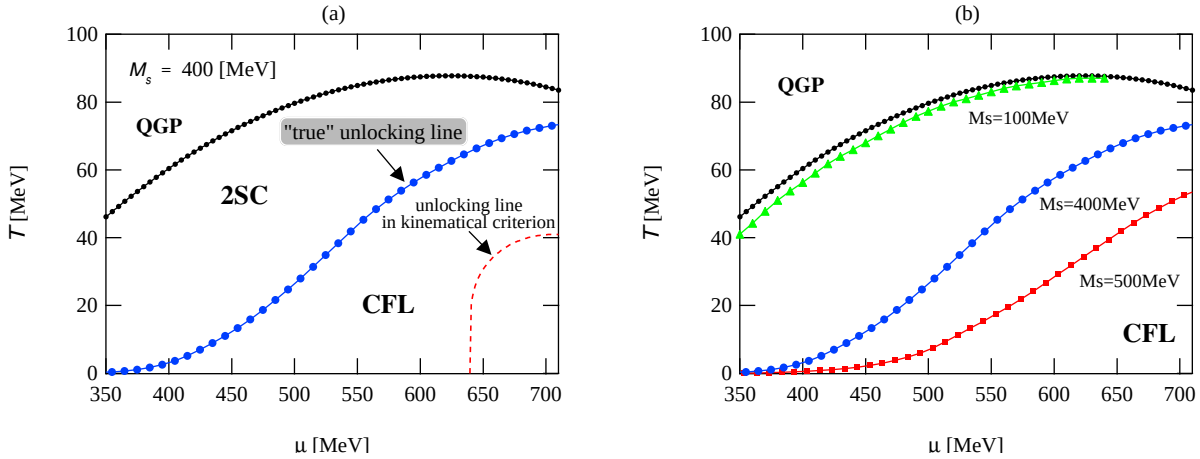

FIG. 8: (a) Phase diagram in (μ, T) plane for $M_s = 400$ MeV. The bold dots represent the phase boundary between the 2SC and QGP phases. This is characterized by 2nd order phase transition. The squares are the color-flavor unlocking line for $M_s = 400$ MeV. This divides the superconducting region into the upper 2SC phase and the lower CFL phase by 2nd order phase transition. The dashed line shows a unlocking line evaluated with a simple kinematical criterion. (b) The color-flavor unlocking lines for $M_s = 100$ MeV (triangles), 400 MeV (bold dots), and 500 MeV (squares).

mass. Though we have not included the usual vacuum effect of chiral symmetry breaking due to non vanishing $\langle\bar{q}q\rangle$, but once it is included, we might have one line in (μ, T) plane, on which the $\bar{q}q$ condensates show singular behaviours [26, 27]. However, this effect enters the superconducting gap equation only through shifts of the quark masses. Let us here suppose that the discontinuity in $\langle\bar{q}q\rangle$ at $T = 0$ occurs at $\mu = \mu_V = 450$ MeV, and that the constituent strange quark mass is about 500 MeV for the chiral broken $\mu < 450$ MeV. Even if instantons are relevant at the chiral restoration point, this would not significantly affect the constituent mass for the strange quark sector. If so, we still might have the dCFL phase, the BEC phase of bound pairs of heavy strange quark and light species for $\mu > \mu_V = 450$ MeV and low T region in the phase diagram, as is easily guessed from the squares in FIG. 8(b). If this is the case, the chiral symmetry is always broken at $T = 0$, regardless of the value of the chemical potential [25].

IV. SUMMARY

In this paper, we have applied the NJL model to study the phases of quark matter under high chemical potential. We have constructed the correct effective potential for multi-gap parameters including color-flavor sextet channels to determine the phase diagram, and which has not yet been taken care in other references. In particular, we have revisited the unlocking phase transition from the CFL to the 2SC. We list main results below.

1. Second order phase transition. The unlocking transition is of continuous weak 2nd order. The 1st order unlocking never appear even at $T = 0$. This contradicts the simple kinematical picture for the color-flavor unlocking transition.

2. Toughness of the CFL state. The CFL state at $T = 0$ is much robuster against the increase of M_s than is predicted from the kinematical criterion, and the 2SC state is continuously connected from the dCFL state at the strange quark mass $M_s^c \& \quad (\quad 2^{\sqrt{\quad}} \overline{\quad}_8(\ ; M_s = 0))$.

3. The 2SC as a saddle point. 2SC state is always a saddle point, a solution of the gap equation, of the effective potential for any value of M_s, which is unstable in the direction towards the dCFL state, as well as three color-flavor sextet directions. The dCFL state, a solution of the gap equation with a larger condensation energy than the 2SC state approaches the 2SC saddle point as M_s approaches M_s^c.

4. Role of the sextet gap parameters. The dCFL state is also unstable in the directions for three color-flavor symmetric channels. This is attributed to the fact that the interaction is repulsive in these channels. We should not include the symmetric components of the gap parameter into our ansatz from the beginning, because no Cooper instability is present in these channels due to the absence of the attractive force. However, the effects of the sextet gaps on the anti-triplet sector are very small even if they are included.

5. Crossover from the BCS to the BEC state. It is indicated from the coincidence of the strange quark mass for the unlocking transition and that for the vanishing strange quark density, that the system undergoes a crossover from the CFL-type BCS state to the Bose-Einsein condensation (BEC) of tightly bound bosonic pairs constituted by strange quark and light flavors with increasing strange quark mass, or equivalently decreasing the density of the strangeness. The binding energy of the pair corresponds to the value of $E_B = M_s^c \quad ,$

and it could be of the order of several hundreds MeV at lowest strange density.

If the scenario of the crossover is exactly the case, the incoherent Bose gas of pairs might exist above the critical temperature for the unlocking $T_c^{unlock} < T < T_c$, and which may provide another description of so-called "pseudogap" phase. In order to confirm this picture, we have to study q-q bound state for finite temperature and density. The Bethe-Salpeter equation would be a good starting point to investigate this crossover phenomenon.

In this paper, we completely neglected the electric charge neutrality and also the color neutrality [28, 29]. It would be interesting to study these effect on the gap equation, and to confirm whether our BEC state is robust or fragile to be withdrawn by the neutrality condition. Also, we have ignored the usual chiral condensates in the vacuum. However, we have to include this effect to discuss the phase transitions in the lower chemical potential region. Studying phase transitions in this regime by improving our model along this line is also an interesting subject to be done in the future.

Acknowledgments

I am grateful to T. Kunihiro for critical advices, stimulating discussions and continuous encouragements. I would also like to express my sincere thanks to T.T. Takahashi, M. Kitazawa, H. Matsufuru, N. Ikezi and S. Nakamura for helpful conversations and warm encouragements, and to K. Iida and M. Tachibana and K. Rajagopal for their valuable comments and interests in this work.

APPENDIX A: GAP EQUATIONS

We summarize here some quantities, in particular, the quark propagators and the resulting dispersion relations of the quasi-quarks, both of which are relevant to the calculation of the gap equation and the effective potential.

Propagators. Iso-triplet and iso-doublet sector of the propagator matrix (Eq. (7)) are

$$R_{83}(p;\ _{83}) = \ _5C\frac{1}{2}\ \frac{\ ^{83}}{p_0^2\quad(p\quad)^2\quad\ ^2_{83}}\ +(\ \$\quad);$$

$$R_{82}(p;\ _{82}) = \ _5C\frac{1}{4}\ \frac{\ ^{82}}{p_0^2\quad(p\quad)^2\quad\ ^2_{82}}+\frac{\ ^{82}}{p_0^2\quad(\ \sqrt{p^2+M_s^2}\quad)^2\quad\ ^2_{82}}\ +(\ \$\quad):$$

The component of iso-singlet mixing sector, namely $R_{81}(\ _{81};\ ;\ _{11})$, $R(\ _{81};\ ;\ _{11})$ and $R_{11}(\ _{81};\ ;\ _{11})$ takes very complicated form. For example, $R_{81}(\ _{81};\ ;\ _{11})$ turns out

$$R_{81}(p;\tilde{}) = \ _5C\ \frac{\ _{81}p_0^6 \quad A_3(p;M_s;\tilde{})p_0^4 \quad A_5(p;M_s;\tilde{})p_0^2 \quad A_7(p;M_s;\tilde{})}{p_0^8 + B_2(p;M_s;\tilde{})p_0^6 + B_4(p;M_s;\tilde{})p_0^4 + B_6(p;M_s;\tilde{})p_0^2 + B_8(p;M_s;\tilde{})}\ ;$$

with

$$\begin{aligned}
A_3(p;M_s;\tilde{};\ ) &= 3\ _{81}(p^2 + \ ^2) + \ _{81}^3 \quad \ ^2\ _{11} + 2\ _{81}(\ ^2 + \ _{11}^2) \\
&\quad + \frac{2}{9}M_s^2\left\{5\ _{81} + \sqrt{2}\ + \ _{11}\right\}; \\
A_5(p;M_s;\tilde{};\ ) &= \quad 3p^4\ _{81} \quad 2p^2\ _{81}^3 \quad \ ^2\ _{11} + \ _{81}(2(\ ^2 + \ _{11}^2) + \ ^2) \\
&\quad + 3\ _{81}^2\ ^2\ _{11} \quad 2\ _{81}^3(\ _{11}^2 + \ ^2) + \ ^2\ _{11}(2\ ^2 + \ _{11}^2 + 2\ ^2) \\
&\quad \ _{81}(\ ^2 + \ _{11}^2 + \ ^2)(\ ^2 + \ _{11}^2 + 3\ ^2) \\
&\quad + \frac{M_s^2}{9}\left\{4p^2(5\ _{81} + \sqrt{2}\ + \ _{11}) \quad 6\ _{81}^2(\sqrt{2}\ + \ _{11})\right. \\
&\quad + \ _{11}(5\ ^2 \quad 2\ _{11}^2 \quad 4\ ^2) \quad 2\sqrt{2} \quad 2\ ^2 + \ _{11}^2 \quad 4\ ^2 \\
&\quad \left. 2\ _{81}^3 \quad 2\ _{81}(5\ ^2 + 4\sqrt{2}\ \ _{11} + 7\ _{11}^2 + 4\ ^2)\right\} \\
&\quad + \frac{M_s^4}{9}\left\{\ _{81} \quad 2(\sqrt{2}\ + \ _{11})\right\}; \\
A_7(p;M_s;\tilde{};\ ) &= (\text{complicated terms of energy}^{\ 7}); \\
B_2(p;M_s;\tilde{};\ ) &= \quad 2\ 2(p^2 + \ ^2)\ _{81}^2 + 2\ ^2 + \ _{11}^2 \quad 2M_s^2; \\
B_4(p;M_s;\tilde{};\ ) &= 6p^4 + 2p^2 \quad 6\ ^2 + 3(\ _{11}^2 + \ _{81}^2) + 2\ ^2 + 6\ ^4 + 6(\ _{11}^2 + \ _{81}^2)\ ^2 \\
&\quad + 6\ ^4 + \ _{11}^4 + 4\ _{11}^2\ _{81}^2 + \ _{81}^4 + 4\ ^2(\ _{11}^2 \quad \ _{11}\ _{81} + \ _{81}^2 + 3\ ^2) \\
&\quad + \frac{2}{9}M_s^2\left\{27p^2 + 9\ ^2 + 26\ ^2 + 13\ _{11}^2 + 4\ _{11}\ _{81} + 10\ _{81}^2\right. \\
&\quad \left. + 4\sqrt{2}\ (2\ _{11} + \ _{81}) \right\} + M_s^4; \\
B_6(p;M_s;\tilde{};\ ) &= (\text{complicated terms of energy}^{\ 6}); \\
B_8(p;M_s;\tilde{};\ ) &= (\text{complicated terms of energy}^{\ 8}):
\end{aligned}$$

These propagators reduce to considerably simple forms in the case of the 2SC state and the pure CFL state. For the 2SC state with $\ _{2SC} = \ 3\ _{81} = \ 3 = \sqrt{2} = \ 3\ _{11}=2$, we have

$$R_{81}(p;\ _{2SC}) = \ _5C\frac{1}{6}\ \frac{\ _{2SC}}{p_0^2 \quad (p \quad)^2 \quad _{2SC}^2} + \frac{\ _{2SC}}{p_0^2 \quad (p \quad)^2 \quad _{2SC}^2}\ ;$$

and $R(p;\ _{2SC}) = \sqrt{2}R_{81}(p;\ _{2SC});\ \ R_{11}(p;\ _{2SC}) = 2R_{81}(p;\ _{2SC})$. These do not depend on the value of M_s. As for the pure CFL state with $M_s = 0;\ _{83} = \ _{82} = \ _{81} \quad \ _8;\ =$

$0;\ _{11} = \ _1$, we obtain $R(p;CFL) = 0$, and

$$R_{81}(p;CFL) = \ _5C\frac{1}{2}\ \frac{8}{p_0^2\ (p\ \ ^2)\ \ _8^2} + \frac{8}{p_0^2\ (p+\ \ ^2)\ \ _8^2}\ ;$$

$$R_{11}(p;CFL) = \ _5C\frac{1}{2}\ \frac{1}{p_0^2\ (p\ \ ^2)\ \ _1^2} + \frac{1}{p_0^2\ (p+\ \ ^2)\ \ _1^2}\ :$$

Fermionic dispersion. Fermionic excitation dispersions can be determined by the poles of the quark propagator. We can easily extract the seven low energy dispersions out of nine as

$$d = 3\ : E_{83} = \sqrt{(p\ \ ^2) + \ _{83}^2}; \tag{A1}$$

$$d = 2\ : E_{82}^0 = \sqrt{(p\ \ ^2) + \ _{82}^2}; \tag{A2}$$

$$d = 2\ : E_{82} = \sqrt{(\ p^2 + M_s^2\ \ \ )^2 + \ _{82}^2}: \tag{A3}$$

$E_{83}; E_{82}^0$ and E_{82} are the dispersion relation for the iso-triplet, iso-doublet, and iso-doublet excitations, respectively, and d represents the degeneracy of each excitation. Other two dispersions cannot be written in such simple forms. However, in principle, they can be obtained by solving

$$z^4 + B_2(p;M_s;\tilde{\ };\ )z^3 + B_4(p;M_s;\tilde{\ };\ )z^2 + B_6(p;M_s;\tilde{\ };\ )z + B_8(p;M_s;\tilde{\ };\ ) = 0 \tag{A4}$$

in variable z from the smallest solution up to two, and putting $E(p) = \sqrt{z}$. There are four solutions in the quadratic equation in general, but other two solutions can be obtained through the procedure $\ !\ $ in the two smaller solution, and which are higher blanches of the dispersions, indeed for the excitation which consist mostly of anti-quarks component.

APPENDIX B: EFFECTIVE POTENTIAL

Here, we explicitly calculate some blocks of the effective potential via the Pauli trick.

Condensation energy. The condensation energy term, the second term of Eq. (36), is hard to calculate the frequency integral except for some blocks. For example, iso-triplet sector, we can calculate as

$$12\int_0^{\ 1} dt\ _{83}R_{83}[\ _{83}t] = 3\int\frac{dq}{(2\ )^3}\int_0^{\ 1} dt\ \sqrt{\frac{t^{\ 2}_{83}}{(q\ \ ^2) + t^2\ ^2_{83}}} + (\ \$\ \ \ \ )$$

$$= 3\int\frac{dq}{(2\ )^3}\ \sqrt{E_0^2 + \ _{83}^2}\ \ \ |E_0| + (\ \$\ \ \ \ ):$$

Here, we have defined the bare quark dispersion $E_M = |\sqrt{q^2 + M^2}|$. In the same manner, iso-doublet sector, we obtain

$$16 \int_0^1 dt\ {}_{82}R_{82}[{}_{82}t] = 2 \int \frac{dq}{(2\ )^3} \sqrt{E_0^2 + {}^2_{82}}\ |E_0| + (\$\quad) = 2 \int \frac{dq}{(2\ )^3} \sqrt{E_{M_s}^2 + {}^2_{82}}\ |E_{M_s}| + (\$\quad):$$

However, it cannot evaluate integral of the singlet mixing sector $R_{81}; R_{\ }; R_{11}$ analytically, thus we calculated these numerically.

Mean field potential. The pure CFL state in Eq. (3) can be written in terms of color-flavor anti-symmetric and symmetric components as following

$$\frac{1}{3}{}^{a\ b}_{i\ j}{}_1 + {}^{a\ b}_{j\ i} \frac{1}{3}{}^{a\ b}_{i\ j}{}_8 = ({}^{a\ b}_{i\ j} + {}^{a\ b}_{j\ i})\ {}_S + ({}^{a\ b}_{i\ j} - {}^{a\ b}_{j\ i})\ {}_A; \tag{B1}$$

with definition:

$${}_A = \frac{1}{6}{}_1 - \frac{2}{3}{}_8; \quad {}_S = \frac{1}{6}{}_1 + \frac{1}{3}{}_8: \tag{B2}$$

In the case of finite strange quark mass, we have two anti-symmetric components and three symmetric components. We can extract these components as following. For (u;d) anti-symmetric part ((u;d) (d;u)), we have

$${}^{ud}_A = -\frac{3}{4}{}_{83} + \frac{1}{12}{}_{81} + \frac{\sqrt{2}}{6} + \frac{1}{6}{}_{11}: \tag{B3}$$

For (u;d) symmetric part ((u;d) + (d;u)),

$${}^{ud}_S = \frac{1}{4}{}_{83} + \frac{1}{12}{}_{81} + \frac{\sqrt{2}}{6} + \frac{1}{6}{}_{11}: \tag{B4}$$

For (u;s) or equivalently (d;s) part, we obtain

$${}^{us(ds)}_A = -\frac{1}{2}{}_{82} - \frac{1}{6}{}_{81} - \frac{\sqrt{2}}{12} + \frac{1}{6}{}_{11}; \tag{B5}$$

$${}^{us(ds)}_S = +\frac{1}{2}{}_{82} - \frac{1}{6}{}_{81} - \frac{\sqrt{2}}{12} + \frac{1}{6}{}_{11}: \tag{B6}$$

For the symmetric 2(u;u) = 2(d;d) sectors,

$${}^{uu(dd)}_S = \frac{1}{4}{}_{83} + \frac{1}{12}{}_{81} + \frac{\sqrt{2}}{6} + \frac{1}{6}{}_{11} - {}^{ud}_S; \tag{B7}$$

which is completely equal to $\langle \bar{s}^{ud}_{S} \rangle$ by the remaining $SU(2)_V$ isospin symmetry. Finally, for $2(s;s)$ sector, we have

$$\langle \bar{s}^{ss}_{S} \rangle = \frac{1}{3}\,\Delta_{81} - \frac{\sqrt{2}}{3} + \frac{1}{6}\,\Delta_{11}: \tag{B8}$$

If we forbid the condensation in the color-flavor symmetric channel, the three independent constraints $\langle \bar{s}^{uu(dd)}_{S} \rangle = \langle \bar{s}^{ss}_{S} \rangle = \langle \bar{s}^{us(ds)}_{S} \rangle = 0$ are to be postulated. These give

$$\Delta_{81} = \frac{1}{3}\,\Delta_{83} + \frac{4}{3}\,\Delta_{82}; \quad = \frac{\sqrt{2}}{3}\,\Delta_{83} + \frac{\sqrt{2}}{3}\,\Delta_{82}; \quad \Delta_{11} = \frac{2}{3}\,\Delta_{83} - \frac{4}{3}\,\Delta_{82}: \tag{B9}$$

And the relation $\langle \bar{s}^{ud}_{A} \rangle = \Delta_{83}; \ \langle \bar{s}^{us}_{A} \rangle = \Delta_{82}$ hold. The quadratic terms in the effective potential, namely the mean field potential in the effective potential can be significantly simplified in terms of Δ_A and Δ_S. We saw above the linear relation

$$\begin{pmatrix} \langle \bar{s}^{ud}_{A} \rangle \\ \langle \bar{s}^{us(ud)}_{A} \rangle \\ \langle \bar{s}^{ud}_{S} \rangle \\ \langle \bar{s}^{us(ds)}_{S} \rangle \\ \langle \bar{s}^{ss}_{S} \rangle \end{pmatrix} = \begin{pmatrix} 3/4 & 0 & 1/12 & \sqrt{2}/6 & 1/6 \\ 0 & 1/2 & 1/6 & \sqrt{2}/12 & 1/6 \\ 1/4 & 0 & 1/12 & \sqrt{2}/6 & 1/6 \\ 0 & 1/2 & 1/6 & \sqrt{2}/12 & 1/6 \\ 0 & 0 & 1/3 & \sqrt{2}/3 & 1/6 \end{pmatrix} \begin{pmatrix} \Delta_{83} \\ \Delta_{82} \\ \Delta_{81} \\ \Delta_{11} \end{pmatrix}: \tag{B10}$$

In this base, the first term in Eq. (36), which is quadratic in the gap parameter, can be diagonalized as

$$\frac{3}{4g^2}(\tilde{\ }; \hat{B}\hat{A}\tilde{\ }) = \frac{12}{g^2}\,\langle \bar{s}^{ud2}_{A} \rangle + 2\,\langle \bar{s}^{us2}_{A} \rangle - 2\,\langle \bar{s}^{ss2}_{S} \rangle - 6\,\langle \bar{s}^{ud2}_{S} \rangle - 4\,\langle \bar{s}^{us2}_{S} \rangle : \tag{B11}$$

Note that the quadratic form is not positive definite. There are three directions in which the effective potential is unstable, corresponding to the color-flavor symmetric channels.

In general, it is hard to evaluate analytically the gap-integral of singlet mixing sector in the formula of the effective potential, Eq. (36). However, as noted in the Sec. IIB, there are two special cases in which we can calculate the gap-integral.

The pure CFL state with $M_s = 0$. This corresponds to the following off-diagonal self-energy Eq. (3). In this case, the effective potential at finite temperature reads

$$[\ \Delta_1; \ \Delta_8; \ ;T] = \frac{3}{g^2}\,\Delta_1(\ \Delta_1 + 8\ \Delta_8) \quad 8E_{cond.}(\ \Delta_8; \ ;T) \quad E_{cond.}(\ \Delta_1; \ ;T); \tag{B12}$$

with the definition

$$E_{cond.}(\ ; \ ;T) = +2 \int \frac{dq}{(2\ )^3} \log \left[\frac{\cosh(\ (q \quad \mu)^2 + \ ^2}{\cosh(|q| \quad |\mu|/2T)} \right] + (\ \$ \quad): \tag{B13}$$

Note that the quadratic term, namely the mean field potential, can be written in the diagonal form as

$$\frac{3}{g^2}\ {}_1(\ {}_1+8\ {}_8)=\frac{36}{g^2}(\ {}^2_A\quad 4\ {}^2_S); \tag{B14}$$

where $_S$ and $_A$ are the symmetric and anti-symmetric component of the gap matrix Eq. (B2). The negative sign in front of ^2_S implies that the effective potential is unbound in the direction of the repulsive channels.

The 2SC state for an arbitrary value of M_s. In the case of the 2SC defined by Eq. (4), the effective potential at finite temperature becomes

$$[\ {}_{2SC};\ ;T;M_s]=\ \frac{12}{g^2}\ {}^2_{2SC}\quad 4E_{cond:}(\ {}_{2SC};\ ;T): \tag{B15}$$

Note that the strange quark mass M_s does not enters this expression.

---

[1] D. Bailin and A. Love, Phys. Rep. 107, 325 (1984),

[2] M. Iwasaki and T. Iwado, Phys. Lett. B 350, 163 (1995); M.G. Alford, K. Rajagopal and F. Wilczek, Phys. Lett. B 422, 247 (1998); R. Rapp, T. Schafer, E.V. Shuryak and M. Velkovsky, Phys. Rev. Lett. 81, 53 (1998).

[3] For reviews, see K. Rajagopal and F. Wilczek, arXiv:hep-ph/0011333; M.G. Alford, Ann. Rev. Nucl. Part. Sci. 51, 131 (2001); T. Schafer, arXiv:hep-ph/0304281; D.H. Rischke, arXiv:nucl-th/0305030.

[4] M.G. Alford, K. Rajagopal and F. Wilczek, Nucl. Phys. B 537, 443 (1999).

[5] T. Schafer and F. Wilczek, Phys. Rev. D 60, 074014 (1999).

[6] M. Alford, J. Berges and K. Rajagopal, Nucl. Phys. B 558, 219 (1999).

[7] A.I. Larkin and Yu.N. Ovchinnikov, Zh. Eksp. Teor. Fiz. 47, 1136 (1964) [Sov. Phys. JETP 20, 762 (1965)]; P. Fulde and R.A. Ferrell, Phys. Rev. 135, A550 (1964);

[8] M.G. Alford, J.A. Bowers and K. Rajagopal, Phys. Rev. D 63, 074016 (2001); J.A. Bowers, J. Kundu, K. Rajagopal and E. Shuster, Phys. Rev. D 64, 014024 (2001); J. Kundu and K. Rajagopal, Phys. Rev. D 65, 094022 (2002); J.A. Bowers and K. Rajagopal, Phys. Rev. D 66, 065022 (2002); R. Casalbuoni and G. Nardulli, arXiv:hep-ph/0305069.

[9] T. Schafer, Phys. Rev. Lett. 85, 5531 (2000); D.B. Kaplan and S. Reddy, Phys. Rev. D 65, 054042 (2002).

[10] I. Shovkovy and M. Huang, Phys. Lett. B 564, 205 (2003); M. Huang and I. Shovkovy, arXiv:hep-ph/0307273.

[11] E. Gubankova, W.V. Liu and F. Wilczek, Phys. Rev. Lett. 91, 032001 (2003); M. Alford, C. Kouvaris and K. Rajagopal, arXiv:hep-ph/0311286.

[12] K. Iida, T. Matsuura, M. Tachibana and T. Hatsuda, arXiv:hep-ph/0312363.

[13] A.J. Leggett, in Modern Trends in the Theory of Condensed Matter (Springer, Berlin, 1980), p.13; J. Phys. (Paris) 41, C7-19 (1980).

[14] P. Nozieres and S. Schmitt-Rink, J. Low Temp. Phys. 59, 195 (1985).

[15] U. Lombardo, P. Nozieres, P. Schuck, H.J. Schulze and A. Sedrakian, Phys. Rev. C 64, 064314 (2001).

[16] M. Matsuzaki, Phys. Rev. D 62, 017501 (2000); H. Abuki, T. Hatsuda and K. Itakura, Phys. Rev. D 65, 074014 (2002).

[17] Y. Nishida, K. Fukushima and T. Hatsuda, arXiv:hep-ph/0306066.

[18] T. Schafer, Nucl. Phys. B 575, 269 (2000).

[19] H. Abuki, Prog. Theor. Phys. 110, 937 (2003).

[20] I.A. Shovkovy and L.C.R. Wijewardhana, Phys. Lett. B 470, 189 (1999).

[21] R. Casalbuoni, R. Gatto, G. Nardulli and M. Ruggieri, Phys. Rev. D 68, 034024 (2003).

[22] V.M. Loktev, R.M. Quick and S.G. Sharapov, Phys. Rept. 349, 1 (2001).

[23] M. Kitazawa, T. Koide, T. Kunihiro and Y. Nemoto, Phys. Rev. D 65, 091504, (2002).

[24] M. Kitazawa, T. Koide, T. Kunihiro and Y. Nemoto, arXiv:hep-ph/0309026; A. Schnell, G. Ropke and P. Schuck, Phys. Rev. Lett. 83, 1926 (1999).

[25] T. Schafer, Phys. Rev. D 62, 094007 (2000).

[26] S.P. Klevansky, Rev. Mod. Phys. 64, 649 (1992); T. Hatsuda and T. Kunihiro, Phys. Rep. 247, 221 (1994).

[27] T. Schafer and E. Shuryak, Rev. Mod. Phys. 70, 323 (1998).

[28] M. Alford and K. Rajagopal, JHEP 0206, 031 (2002); A.W. Steiner, S. Reddy and M. Prakash, Phys. Rev. D 66, 094007 (2002); F. Neumann, M. Buballa and M. Oertel, Nucl. Phys. A 714, 481 (2003).

[29] K. Iida and G. Baym, Phys. Rev. D 63, 074018 (2001).